

High brightness and high polarization electron source using transmission photocathode with GaAs-GaAsP superlattice layers

Naoto Yamamoto,^{1,a)} Tsutomu Nakanishi,^{1,b)} Atsushi Mano,¹ Yasuhide Nakagawa,¹ Shoji Okumi,¹ Masahiro Yamamoto,¹ Taro Konomi,¹ Xiuguang Jin,² Toru Ujihara,² Yoshikazu Takeda,² Takashi Ohshima,³ Takashi Saka,⁴ Toshihiro Kato,⁵ Hiromichi Horinaka,⁶ Tsuneo Yasue,⁷ Takanori Koshikawa,⁷ and Makoto Kuwahara⁸

¹Graduate School of Science, Nagoya University, Nagoya 464-8602, Japan

²Graduate School of Engineering, Nagoya University, Nagoya 464-8603, Japan

³Central Research Laboratory, Hitachi Ltd., Tokyo 185-8601, Japan

⁴Daido Institute of Technology, Nagoya 457-8531, Japan

⁵Daido Steel Co. Ltd., Nagoya 457-8531, Japan

⁶Faculty of Engineering, Osaka Prefecture University, Osaka 599-8531, Japan

⁷Fundamental Electronics Research Institute, Osaka Electro-Communication University, Osaka 572-8530, Japan

⁸Research Institute of Electrical Communication Tohoku University, Sendai 980-8577, Japan

(Received 23 October 2007; accepted 21 December 2007; published online 20 March 2008)

In order to produce a high brightness and high spin polarization electron beam, a pointlike emission mechanism is required for the photocathode of a GaAs polarized electron source. For this purpose, the laser spot size on the photocathode must be minimized, which is realized by changing the direction of the injection laser light from the front side to the back side of the photocathode. Based on this concept, a 20 kV gun was constructed with a transmission photocathode including an active layer of a GaAs–GaAsP superlattice layer. This system produces a laser spot diameter as small as $1.3 \mu\text{m}$ for 760–810 nm laser wavelength. The brightness of the polarized electron beam was $\sim 2.0 \times 10^7 \text{ A cm}^{-2} \text{ sr}^{-1}$, which corresponds to a reduced brightness of $\sim 1.0 \times 10^7 \text{ A m}^{-2} \text{ sr}^{-1} \text{ V}^{-1}$. The peak polarization of 77% was achieved up to now. A charge density lifetime of $1.8 \times 10^8 \text{ C cm}^{-2}$ was observed for an extracted current of $3 \mu\text{A}$. © 2008 American Institute of Physics. [DOI: 10.1063/1.2887930]

I. INTRODUCTION

The GaAs-type semiconductor photocathode (PC) with a negative electron affinity (NEA) surface is currently used as a conventionally polarized electron source (PES) to produce a highly polarized electron beam. The PES is based on two fundamental physical processes: (1) optical spin orientation at band-gap excitation and (2) electron emission through the surface potential barrier due to the NEA surface. In a conventional PC scheme, circular polarized laser light is injected from the NEA surface side and the electrons are extracted to the same side. Polarized electron beams produced by conventional NEA-PC have been widely used in high energy electron accelerators for spin physics studies of fundamental particles or hadrons.^{1–6} They have also been employed in low energy electron microscopes (LEEMs) for surface spin physics of magnetic materials, such as spin low energy electron microscopy (SPLEEM).⁷

To answer the urgent needs of future high energy accelerators such as the International Linear Accelerator (ILC),⁸ several groups, including our own, have made long-term efforts to improve PES (PC+gun) performances, including polarization, quantum efficiency, and beam emittance. For example, electron spin polarization (ESP) higher than 85% has been achieved by strained GaAs (Ref. 9) and GaAs–GaAsP

strained super-lattice (SL) layers¹⁰ grown on a GaAsP buffer substrate. A quantum efficiency (QE) higher than 0.3% has been simultaneously obtained for the same PCs.

Futhermore, extremely low emittance of electron beams are required for accelerator-based x-ray sources of energy recovery linac (ERL) projects.^{11–13} Polarization is not necessary in this case, but the NEA-PC has a well-known advantage of offering a small energy spread in the source beam. We have recently demonstrated experimentally that normalized-rms thermal (or initial) emittance can be minimized to as low as $0.15\pi \text{ mm mrad}$ for a beam radius of 1.0 mm, by using a GaAs–GaAsP strained SL layer PC installed in a 200 kV dc gun.¹⁴ Based on this result, the high field gradient dc gun (bias voltage $\geq 500 \text{ kV}$) with a SL-PC is now considered to be highly suitable for ERL electron sources.

High brightness is one of the most important PES performances for the application to electron microscopes. Several types of pointlike sources have already been developed to produce a needlelike beam, although it cannot produce a polarized beam. Field emission (FE) sources can realize the highest brightness (10^8 – $10^9 \text{ A cm}^{-2} \text{ sr}^{-1}$) and have been used for high space-resolution electron microscopes, such as scanning electron microscopes (SEM) where the radius of the W tip is typically shaped to be as small as 100 nm.

We have recently investigated a similar method, where photoexcited polarized electrons are extracted from a small area tip ($\sim 25 \text{ nm}$ radius) of pyramidal-shaped GaAs. The

^{a)}Electronic mail: naoto@spin.phys.nagoya-u.ac.jp.

^{b)}Electronic mail: nakanisi@spin.phys.nagoya-u.ac.jp.

estimated brightness is high ($\sim 10^7$ A cm $^{-2}$ sr $^{-1}$) and the observed ESP spectrum is similar to that of NEA bulk-GaAs PC, exhibiting 20%-38% polarization under irradiation with circular polarized light of 700–860 nm.¹⁵ However, this GaAs-tip PC has a clear disadvantage in that the extracted current is limited to less than ~ 20 nA due to tip melting.

Another type of electron source for microscopes is the LaB $_6$ thermionic-emitter with a single crystal tip of radius typically larger than ~ 10 μ m. This source produces a lower brightness (10^5 – 10^6 A cm $^{-2}$ sr $^{-1}$) and is not polarized, but it has a higher total current and the longer lifetime compared with W-tip emitters. It is popularly used for SEMs, transmission electron microscopes (TEM) and LEEMs.

Another SEM source using a NEA-GaAs PC was developed to produce small energy spread beams by one of the coauthors (T. Ohshima).¹⁶ In order to form a small diameter electron beam, laser light is injected from the back surface of a GaAs film grown on a glass sheet, with the excited electrons emitted into vacuum from the front NEA surface of the PC. Using this laser injection scheme, it is possible to decrease the distance between a focusing lens and the PC crystal and to minimize the laser spot size. Hereafter, we distinguish this PC from conventional PCs, by naming them “transmission PC (T-PC)” and “reflection PC (R-PC),” respectively. With a T-PC, a 2 kV gun can produce a needlelike beam with a source diameter of 3 μ m, angular current density of 41 mA/sr and brightness of $\sim 10^6$ A cm $^{-2}$ sr $^{-1}$, where the current density is limited not by the space charge effect, but by the surface charge effect.¹⁷

Recently, LEEM has attracted interest as a powerful tool in surface science due to its ability to perform real-time imaging of metal film surfaces during its growth with a 10 nm space resolution,¹⁸ using a LaB $_6$ emitter as the standard source. SPLEEM is also currently available as an option for a LEEM system, which enables the observation of nanometer scale magnetic domains.^{19,20} However, real-time imaging is not possible using an SPLEEM apparatus, because present PES guns use R-PCs of bulk-GaAs thick layers with a beam brightness of only $\sim 10^4$ A cm $^{-2}$ sr $^{-1}$ and ESP of $\sim 30\%$. This brightness is less than that of a LaB $_6$ emitter by two to three orders of magnitude, and thus a new PES system with higher brightness and higher ESP is urgently required.

The interference between the laser and electron beam lines in the conventional R-PC scheme is a serious problem for gun design and imposes a serious limit on beam performance. For example, it is not easy to replace the unpolarized gun of an electron microscope by a PES gun with a R-PC, because the laser light must be injected in the downstream of the electron beam line to irradiate the R-PC surface.

We have found that this problem can be solved by replacing the conventional R-PC gun by a T-PC gun, whose conceptual scheme is shown in Fig. 1. The interference problem disappears in this T-PC scheme and it becomes possible to set a focusing lens at the back of the T-PC with a small separation. This T-PC scheme appears promising for applications of polarized beam in various types of high energy electron accelerators and microscopes, since there is sufficient

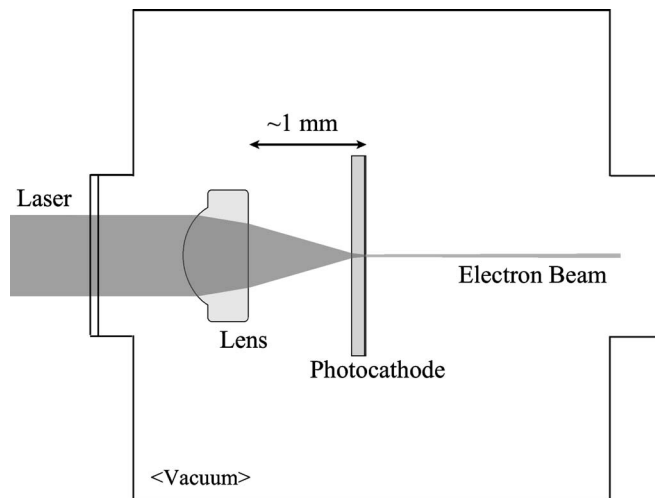


FIG. 1. Conceptual view of a PES gun with a T-PC.

free spaces along both the laser and electron beam lines to enable the optimization of design figures and parameters individually.

A 20 kV gun system (named JPES-1) was designed and built to install the newly designed T-PC at Nagoya University. This new PES system has already achieved a much higher brightness of 2×10^7 A cm $^{-2}$ sr $^{-1}$ and higher ESP value of 77% than those of the available SPLEEM gun. In this article, the details of the experimental methods and results of beam performance measurements on ESP, QE, and brightness are described.

II. EXPERIMENTAL SETUP

A. 20 kV electron gun

JPES-1, the first T-PC PES system, was designed and built at Nagoya University as a prototype SPLEEM gun to demonstrate its high brightness performance. A second T-PC PES system (named JPES-2) is also being designed for installation in the LEEM apparatus operated at Osaka Electro-Communication University (OECU).

JPES-1 consists of five chambers: (1) a NEA surface preparation chamber, (2) a gun chamber, (3) a brightness measuring chamber, (4) a spherical condenser chamber, and (5) a 100 keV Mott polarimeter chamber.²¹ A schematic view of parts (2), (3), and (4) are shown in Fig. 2, the extraction voltage of the gun was chosen to be 20 kV, the voltage at which the LEEM at OECU is operated.

Two important apparatus performances must be met for a high voltage PES gun: (1) an extremely high vacuum ($\leq 10^{-10}$ Pa) environment around the NEA-PC and (2) an extremely low dark current (≤ 10 nA) between the high voltage electrodes. These performances are required to protect the NEA surface and reduce its degradation speed to maintain a long PC lifetime (\geq several tens of hours). Special techniques were employed for this purpose, as will be described in a separate paper.²²

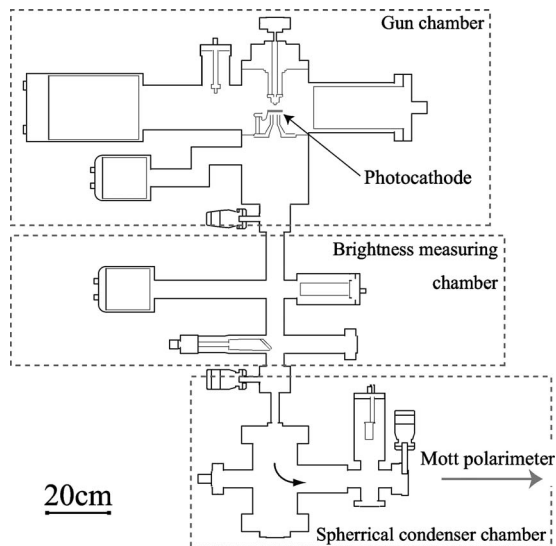


FIG. 2. Schematic view of the 20 kV JPES-1 system.

B. Laser system

A schematic view of the laser optical system is shown in Fig. 3, where a Nd:YVO₄ pumped Ti:sapphire laser (wavelength 700–860 nm) was used as a cw light source, and the light was transmitted to a T-PC installed in the gun chamber by an optical single mode fiber. A polarizing beam splitter is mounted at the exit of the fiber to give linearly polarized light, which is converted to circularly polarized light by a quarter wave plate. The light is then focused on the T-PC surface using an aspherical lens. The position of the lens is adjusted by monitoring the spot size of the reflected light from the T-PC by projecting a magnified focus image of the spot on a charge coupled device (CCD) camera.

An example spot image is shown in Fig. 4, where x and y are the orthogonal axes of the CCD image. This spatial profile was well approximated by a Gaussian distribution function with a radius of $0.65 \mu\text{m}$ half width at half maximum (HWHM). The smallest spot size is near the diffraction limit of 780 nm wavelength light.

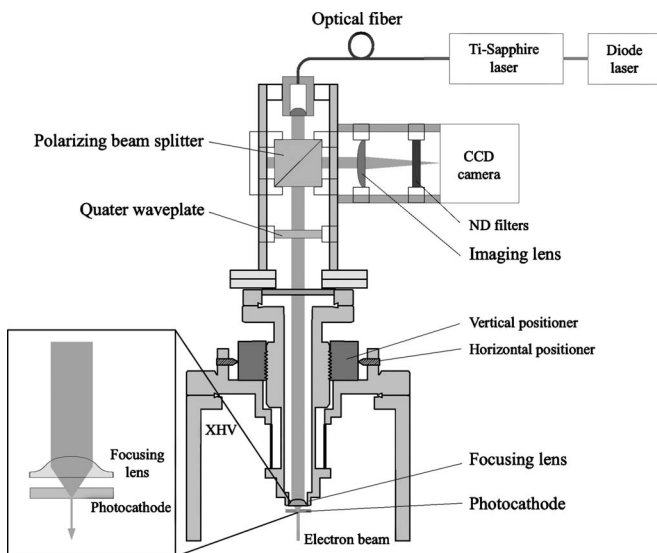


FIG. 3. Schematic view of the laser optical system.

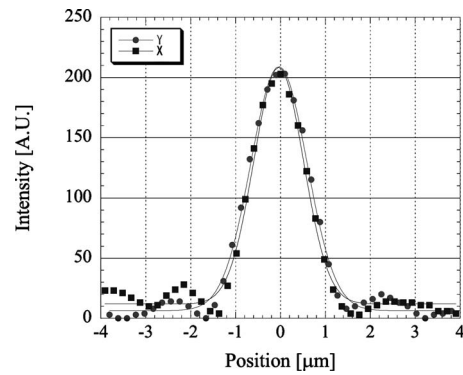


FIG. 4. Typical laser spot profile observed by a CCD camera.

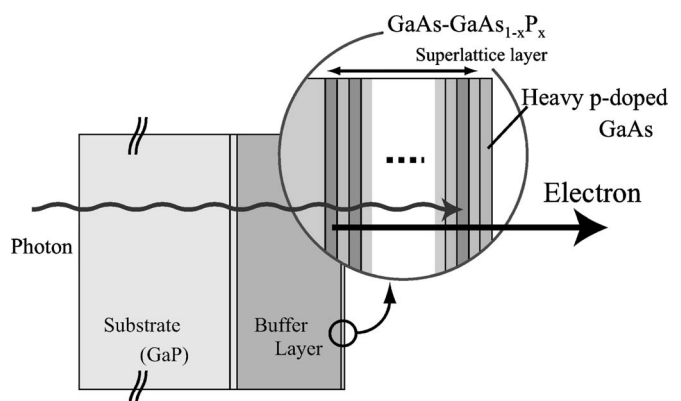
C. Photocathode

A typical crystal layer structure of a T-PC, shown in Fig. 5, was designed to have the same SL structure as that used in the R-PC mode. It consists of substrate, buffer, and active layers. As shown in the enlarged figure, a strained SL structure of 12 pairs of GaAs and GaAsP layers was employed as the active layer to produce polarized electrons in the conduction band. The SL layers was terminated by a heavily Zn doped GaAs surface layer to make a narrow width band-bending region. This design effectively overcomes the surface charge limit effect that appears in the generation of a high current density beam^{17,23} and exhibits ESP and QE performances, as high as 92% and 0.5%, respectively.²⁴

For the T-PC design, the same SL layer structure is employed as for the R-PC. However, the substrate material is changed, since the materials used for the R-PC are not transparent for 780 nm excitation laser light. As a first choice, a commercially available GaP wafer with high Zn doping of $1.4 \times 10^{17} \text{ cm}^{-3}$ was employed instead of a GaAs wafer. The samples in this paper were fabricated by a metal-organic vapor phase epitaxy (MOVPE) apparatus. After fabrications, their crystalline qualities were checked by x-ray diffraction and photoluminescence measurements.

D. Beam performance measuring system

The JPES-1 can measure three kinds of beam performances.

FIG. 5. Schematic crystal layer structure of a T-PC, where x is the fraction ratio of P element in the GaAsP layer.

1. Emission current and quantum efficiency

The emission current and quantum efficiency are measured by the following procedure. The T-PC is heat cleaned at 420–550 °C in the activation chamber and the GaAs surface is activated by deposition of small amounts of Cs and O₂. The QE in the R-PC mode is monitored by simultaneous measurements of photocurrent (total current emitted from the cathode) and laser irradiation power. Then the T-PC is transferred from the activation chamber to the gun chamber by a transporter. It is locked at the center of the cathode electrode and the QE in operation mode is measured by applying an extraction voltage and irradiating the T-PC from the back.

2. Polarization measuring system

The ESP is measured using a standard 100 kV Mott polarimeter.²¹ A 90° bend spherical condenser (radius: of 50 mm and gap length of 5 mm) is used to change the longitudinal spin polarization to a transverse polarization. The Mott polarimeter has four different Au-foil targets of different thickness for self-calibration of the effective Sherman functions. The systematic error for the ESP measurement was estimated to be ±6% (absolute value) at maximum.

3. Brightness measuring system

The beam profile is measured using a pair of knife-edge slits and a Faraday cup installed at the brightness measuring chamber. The angular current density ($dI/d\Omega$) and reduced brightness (B_r) of the electron beam are calculated by the following equations:

$$\frac{dI}{d\Omega} = I \frac{L^2}{\pi(S_L - S_o)^2}, \quad (1)$$

$$B_r = \frac{1}{\pi S_o^2} \frac{dI}{d\Omega} \frac{1}{U}. \quad (2)$$

Here, L is the drift length between the source and the above brightness monitor (BM), and S_o is the beam source radius at the PC surface. S_L and I represent the beam radius and current measured by the BM, and U is the beam energy.

In our apparatus L was chosen to be 53.1 cm. For S_o , a virtual source size must be employed due to the beam focusing property caused by the electrode design, and it was estimated to be about 70% smaller than the emission area of the T-PC. S_L is defined as the width (HWHM) obtained by a numerical fit of the measured beam profile.

The error of our brightness measurement was dominated by the uncertainty of S_o determination. The laser spot size could be well measured as shown in Fig. 4, but the electron emission area was enlarged due to the diffusion effect inside the T-PC. The diffusion effect is considered to be small, because the active SL layer was thin ($\sim 0.1 \mu\text{m}$) compared with the diffusion length of $0.5 \mu\text{m}$ for photoelectrons in heavily p -doped GaAs.^{25,26} In this paper, we assume that the diffusion length in the T-PC is $0.25 \mu\text{m}$.

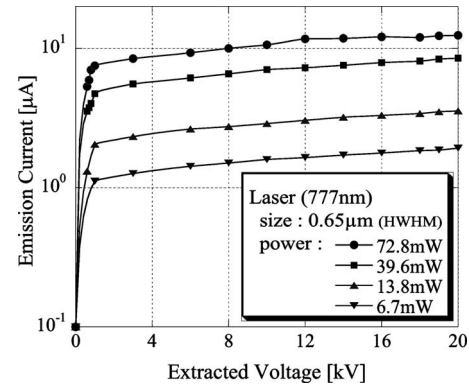


FIG. 6. Emission current as a function of extraction voltage for different laser power conditions.

III. RESULTS AND DISCUSSIONS

The experimental beam performance measurement results are described in this section.

A. Emission current

In Fig. 6, the total emission current emitted from the NEA-PC is plotted as a function of the extraction voltage for several laser irradiation powers. Each curve has a steep rising behavior at the threshold region and a gradually increasing behavior caused by the Schottky effect. Saturation is not evident up to currents over $10 \mu\text{A}$, showing that the space charge limit effect does not dominate the current density under these experimental conditions.

The dependence of the total emission current on the laser power was measured for two QE conditions, as shown in Fig. 7, where the data points with closed circles and open squares indicate QEs of 0.04% and 0.02%, respectively. The radius of the laser spot in this measurement was fixed to be $0.65 \mu\text{m}$ (HWHM) at a wavelength of 807 nm. Both emission currents increase linearly with laser power up to 150 mW, demonstrating that there is no observable evidence of the surface charge limit effect for this range of laser conditions. Assuming that the diffusion length for photoelectrons in the T-PC is $0.25 \mu\text{m}$, the beam radius on the T-PC surface was estimated to be $0.90 \mu\text{m}$. Thus a maximum PC current density of 5.1 A/mm^2 was recorded for the NEA surface condition with a QE of 0.04%. This current density is higher

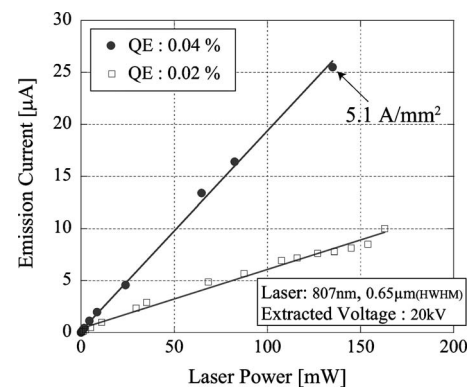


FIG. 7. Emission current as a function of laser power for two different QE surface conditions.

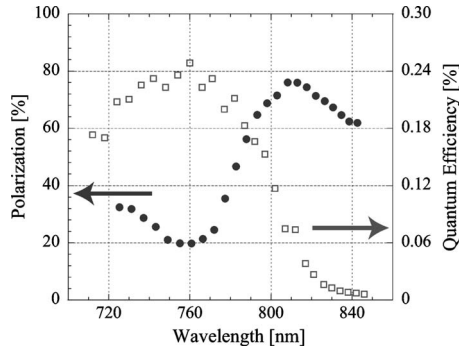


FIG. 8. Observed ESP and QE spectra, indicated by closed circles and open squares, respectively.

than that obtained by a conventional GaAs-GaAsP SL layer in the R-PC mode by one order of magnitude.^{27–29}

The beam lifetime performance was also monitored during the experiments keeping extremely low vacuum pressure ($\leq 2 \times 10^{-9}$ Pa) and extremely low dark current (≤ 1 nA) conditions. As typical data, an initial current of $3 \mu\text{A}$ extracted by $3.2 \mu\text{m}$ radius laser irradiation decreased exponentially with a lifetime of 36 h, which corresponds to a charge lifetime density of $1.8 \times 10^8 \text{ C/cm}^2$. The details of the NEA lifetime performance of JPES-1 will be reported in a forthcoming paper.²²

B. ESP and QE

Examples of ESP and QE spectra taken for a T-PC are shown in Fig. 8, where the closed circle and open square points indicate ESP and QE, respectively. The significant trends are (1) the QE threshold corresponds to the band gap energy ($1.54 \text{ eV} = 807 \text{ nm}$), (2) the peak of the ESP is in the QE threshold region. A maximum ESP of 77% with QE of 0.08% has been achieved by this PC sample at a wavelength of 807 nm. This polarization value is high compared with that of $\sim 30\%$ ESP of the available SPLEEM gun.

For a more detailed ESP analysis, spin-resolved QE spectra²⁴ were derived, as shown in Fig. 9. The spectra were reduced using the following definition formula: $Q_L = \text{QE}(1 + \text{ESP})/2$ and $Q_R = \text{QE}(1 - \text{ESP})/2$, where subscripts *L* and *R* mean left-handed and right-handed electrons. These Q_L and Q_R are proportional to the photoabsorption coefficients be-

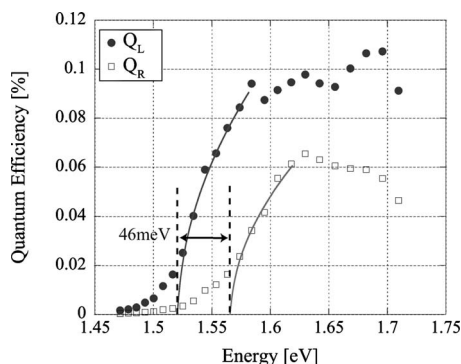


FIG. 9. Spin-resolved QE spectra as a function of laser photon energy, where Q_L and Q_R are indicated by closed circles and open circles, respectively.

tween the miniband at the conduction-band minimum and the heavy-hole (HH) and light-hole (LH) minibands at the valence-band maximum.

The QE spectra in Fig. 8 were converted to spin-resolved QE spectra, shown in Fig. 9, where both solid curves represent numerical fits of the Q_L and Q_R data at the threshold region with a square-root function.

As already mentioned, this T-PC sample was designed to have the same GaAs-GaAsP SL structure as that used in the R-PC mode, for which the ESP is higher than 85%, with an energy splitting of $\sim 70 \text{ meV}$ between the HH and LH bands.²⁴ However, the energy splitting of $\sim 46 \text{ meV}$ obtained in Fig. 9 is smaller than that of the R-PC. In general, a smaller energy splitting results in a smaller ESP, since the overlap of the Q_L and Q_R spectra becomes significant. The discrepancy between the ESP data has been studied by comparing the crystal qualities of each of the sample layers, and further efforts have been made in designing new T-PC samples with an ESP greater than 85%. Detailed descriptions of T-PC developments will be given in a forthcoming paper.³⁰

Under the laser focusing conditions used, the laser beam radius and lens focal length had comparable magnitudes, and the Rayleigh length was estimated to be a few micrometers for 807 nm wavelength. In this case, irradiating of the PC is approximated not by a plane wave but by a parabolic or spherical wave. Therefore, the influence of the irradiation condition on the ESP was checked by changing the laser focus position in a vertical range of 2 mm, as shown in Fig. 10(a), where the positive vertical position ($z \geq 0$) indicates the over-focus condition. As shown in Fig. 10(b), no strong ESP variations were observed, and it is concluded that the influence of the laser focusing condition is negligibly small in our experimental conditions.

C. Brightness

The beam profile was measured using a pair of knife-edge slits located 53.1 cm downstream from the T-PC. The beam radius (HWHM) was determined by Gaussian fitting of the profile data and is shown to be a function of the extraction voltage in Fig. 11(a). The data were taken under a constant emission current of $8.5 \mu\text{A}$ with a constant laser spot size of $0.65 \mu\text{m}$.

The beam radius gradually decreases with increasing the extraction voltage, since the beam diversion effect due to space charge force is inversely proportional to the beam energy. A minimum beam radius was obtained at 20 kV and a half emission angle, defined as the standard deviation of the angular beam distribution, was estimated to be 1.2 mrad.

The reduced brightness can be derived from the beam radius and other parameters by using Eq. (2) of the previous section. The results are shown in Fig. 11(b). The brightness increases gradually and saturates beyond 10 kV. This shows that the gun can be operated at beam energies greater than 10 keV without degradation of the beam brightness. The reduced brightness at 20 kV with $8.5 \mu\text{A}$ was $(0.9 \pm 0.3) \times 10^7 \text{ A m}^{-2} \text{ sr}^{-1} \text{ V}^{-1}$, which corresponds to an absolute brightness of $(1.9 \pm 0.8) \times 10^7 \text{ A cm}^{-2} \text{ sr}^{-1}$.

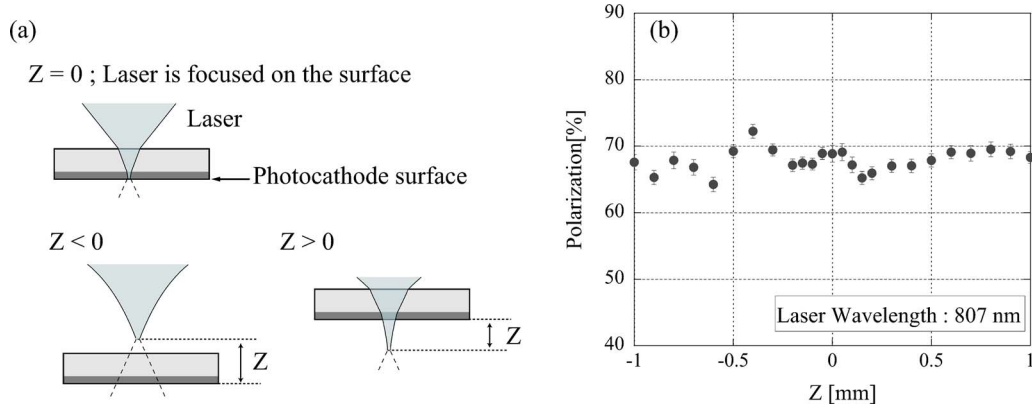


FIG. 10. (Color online) (a) Schematic images of different laser focus conditions along the vertical (z) axis and (b) ESP dependence on laser focus position on z axis.

The brightness dependence on the beam current was also studied at 20 kV by using the same method, with the beam radius kept at 0.95–1.00 mm. As shown in Fig. 12, the brightness increases as the beam current increases, since the angular current density in Eq. (1) of the previous section increases. In this measurement, an angular current density of 248 mA/sr and a reduced brightness of $(1.0 \pm 0.4) \times 10^7 \text{ A m}^{-2} \text{ sr}^{-1} \text{ V}^{-1}$ were obtained at a maximum beam current of 5.3 μA .

This brightness is three orders of magnitude higher than those of the available SPLEEM gun. It is also large compared with those of unpolarized electron emitters. It is smaller than those of W-tip emitters, but a little bit higher than those of LaB₆ emitters.

In NEA-GaAs emitters, the electrons excited to the conduction minimum drift to the surface, tunnel through the narrow barrier at the NEA surface, and escape into vacuum. Therefore, the energy spread of electron beams emitted by this mechanism is considered to be as small as the lattice thermal energy (in our case, at room temperature). This prediction has already been confirmed by various methods^{31,32} including ours.¹⁴ Therefore we concluded that the smallest laser spot realized by the T-PC scheme and the smallest energy spread by the NEA-surface effect play dominant roles in achieving a high brightness in our PES gun system.

IV. SUMMARY

In order to achieve high brightness and high polarization performances for polarized electron beams, the T-PC gun scheme was proposed and a prototype 20 kV gun (JPES-1) was built to demonstrate its advantages. Various types of T-PC samples with active strained SL layers of GaAs–GaAsP and a GaP substrate were fabricated and tested. As preliminary results, the following performances were achieved:

- (1) A small laser spot radius near the diffraction limit (0.65 μm) was obtained on the active T-PC layer.
- (2) A high ESP of $77 \pm 6\%$ was obtained for 807 nm laser irradiation.
- (3) A high current density of 5.1 A/mm² was obtained with no surface charge limit effect.
- (4) A high reduced brightness of $(1.0 \pm 0.4) \times 10^7 \text{ A m}^{-2} \text{ sr}^{-1} \text{ V}^{-1}$ with a high angular current density of 248 mA/sr was obtained with an extracted current of 5.3 μA .
- (5) A long lifetime of $1.8 \times 10^8 \text{ C cm}^{-2}$ was obtained for a beam current of 3 μA by using an extreme high vacuum (XHV) gun chamber.

These performances are better in brightness by three orders of magnitude and in ESP by a factor of 3, compared

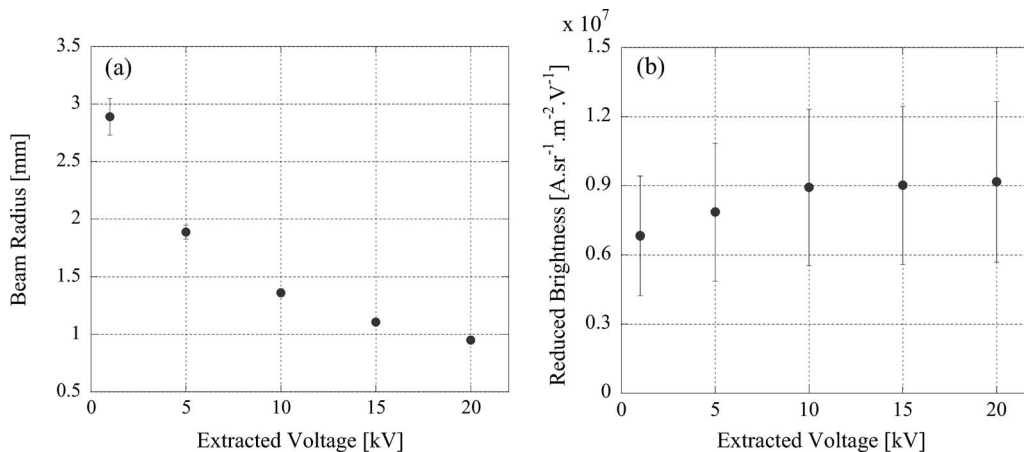


FIG. 11. (a) Beam radius at 63.1 cm downstream from the T-PC and (b) reduced brightness, measured as a function of extraction voltage.

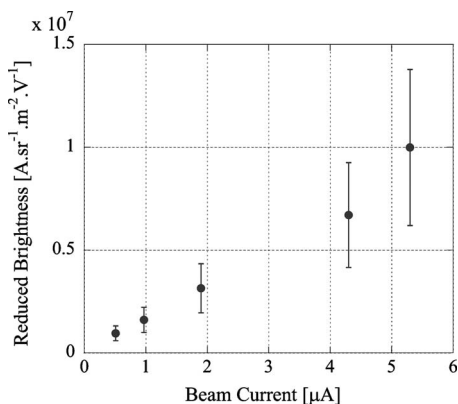


FIG. 12. Reduced brightness as a function of the obtained downstream beam current.

with those achieved by the available SPLEEM gun. Therefore, the advantages of the PES gun with a T-PC are well established by this work. The gun offers the possibility of observing nanometer size magnetic domains in real time, replacing the LaB₆ emitter by this T-PC polarized electron emitter. Encouraged by these results, design work has begun on a second gun (JPES-2), planned to be installed in the LEEM apparatus operated at OECU.

As further applications in other research fields, this PES gun is considered to have many promising possibilities. For example, it can supply highly polarized electrons not only for LEEM but also for other TEM-type microscopes without the serious degradation of beam brightness exhibited by unpolarized LaB₆ emitters. It can also supply electron beams for ERL projects and other high energy accelerators, since both requirements of low emittance and high emission currents can be satisfied by this gun.

ACKNOWLEDGMENTS

The authors wish to thank Professor (emeritus) Y. Kimura, Professors Y. Kamiya, K. Yokoya, M. Yoshioka, and H. Matsumoto of KEK and Professor (emeritus) H. Kobayakawa of Nagoya University for their continuous encouragements of our polarized electron source research project. This work has been financially supported by Japan Science and Technology (JST) as a technology development program for advanced measurement and analysis (program leader: T. Nakanishi). One of the authors (N.Y.) is financially supported by a JSPS Research fellowship for young scientists.

- ¹D. T. Pierce, F. Meier, and P. Zürcher, *Appl. Phys. Lett.* **26**, 670 (1975).
- ²C. Y. Prescott, W. B. Atwood, R. L. A. Cottrell, H. DeStaebler, E. L. Garwin, A. Gonidec, R. H. Miller, L. S. Rochester, T. Sato, D. J. Sherden, C. K. Sinclair, S. Stein, R. E. Taylor, J. E. Clendenin, V. W. Hughes, N. Sasao, K. P. Scholer, M. G. Borghini, K. Lubelsmeyer, and W. Jentschke, *Phys. Lett. B* **77**, 347 (1978).
- ³M. Meyerhoff, D. Eyl, A. Frey, H. G. Andresen, J. R. M. Annand, K. Aulenbacher, J. Becker, J. Blume-Werry, Th. Dombo, R. Drescher, J. E. Ducret, H. Fischer, R. Grabmayr, S. Hall, R. Hartmann, T. Hehl, W. Heil, J. Hoffmann, J. D. Kellie, F. Klein, M. Leduc, H. Moller, Ch. Nachtigall, M. Ostrick, E. W. Otten, R. O. Owens, S. Plitzer, E. Reichert, D. Rohe, M. Schafer, L. D. Scheerer, H. Schmieden, K.-H. Steffens, R. Surkau, and Th. Walcher, *Phys. Lett. B* **327**, 201 (1994).
- ⁴SLD collaboration, K. Abe, I. Abt, C. J. Ahn, T. Akagi, W. W. Ash, D.

- Aston, N. Bacchetta, K. G. Baird, C. Baltay, H. R. Band *et al.*, *Phys. Rev. Lett.* **74**, 2880 (1995).
- ⁵S. Mayer and J. Kessler, *Phys. Rev. Lett.* **74**, 4803 (1995).
- ⁶U. Kolac, M. Donath, K. Ertl, H. Liebl, and V. Dose, *Rev. Sci. Instrum.* **59**, 1933 (1988).
- ⁷E. Bauer, *Rep. Prog. Phys.* **57**, 895 (1994).
- ⁸ILC collaboration (2007), ILC Global Design Effort and World Wide Study (URL <http://lcdev.kek.jp/RDR/>).
- ⁹T. Nakanishi, H. Aoyagi, H. Horinaka, Y. Kamiya, T. Kato, S. Nakamura, T. Saka, and M. Tsubata, *Phys. Lett. A* **158**, 345 (1991).
- ¹⁰T. Nakanishi, K. Togawa, T. Baba, F. Furuta, H. Horinaka, T. Kato, Y. Kurihara, H. Matsumoto, T. Matsuyama, T. Nishitani, S. Okumi, T. Omori, T. Saka, C. Suzuki, Y. Takeuchi, K. Wada, K. Wada, M. Yamamoto, and M. Yoshioka, *Nucl. Instrum. Methods Phys. Res. A* **455**, 109 (2000).
- ¹¹S. M. Gurner, D. Bilderback, I. Bazarov, K. Finkelstein, G. Krafft, L. Merminga, H. Padamsee, Q. Shen, C. Sinclair, and M. Tigner, *Rev. Sci. Instrum.* **73**, 1402 (2002).
- ¹²K. Hirano, *Mater. Res. Soc. Jpn.* **23**, 43 (2003).
- ¹³W. Flavell, E. Seddon, P. Weightman, M. Chesters, M. Poole, F. Quinn, D. Clarke, J. Clarke, and M. Tobin, *J. Phys.: Condens. Matter* **16**, S2405 (2004).
- ¹⁴N. Yamamoto, M. Yamamoto, M. Kuwahara, R. Sakai, T. Morino, K. Tamagaki, A. Mano, A. Utsu, S. Okumi, T. Nakanishi, M. Kuriki, C. Bo, T. Ujihara, and Y. Takeda, *J. Appl. Phys.* **102**, 024904 (2007).
- ¹⁵M. Kuwahara, T. Nakanishi, S. Okumi, M. Yamamoto, M. Miyamoto, N. Yamamoto, K. Yasui, T. Morino, R. Sakai, K. Tamagaki, and K. Yamaguchi, *Jpn. J. Appl. Phys., Part 1* **45**, 6245 (2006).
- ¹⁶T. Ohshima and M. Kudo, *Jpn. J. Appl. Phys., Part 1* **43**, 8335 (2004).
- ¹⁷K. Togawa, T. Nakanishi, T. Baba, F. Furuta, H. Horinaka, T. Ida, Y. Kurihara, H. Matsumoto, T. Matsuyama, M. Mizuta, S. Okumi, T. Omori, C. Suzuki, Y. Takeuchi, K. Wada, K. Wada, and M. Yoshioka, *Nucl. Instrum. Methods Phys. Res.* **414**, 431 (1998).
- ¹⁸J. Chemlik, L. Veneklasen, and G. Marx, *Optik (Stuttgart)* **83**, 155 (1989).
- ¹⁹H. Pinkvos, E. Bauer, H. Poppa, and J. Hurst, *Ultramicroscopy* **47**, 339 (1992).
- ²⁰K. L. Man, R. Zdyb, S. F. Huang, T. C. Leung, C. T. Chan, E. Bauer, and M. S. Altman, *Phys. Rev. B* **67**, 184402 (2003).
- ²¹T. Nakanishi, K. Dohmae, S. Fukui, Y. Hayashi, I. Hirose, N. Horinaka, T. Ikoma, Y. Kamiya, M. Kurashina, and S. Okumi, *Jpn. J. Appl. Phys., Part 1* **25**, 766 (1986).
- ²²S. Okumi *et al.* (unpublished).
- ²³T. Maruyama, A. Brachmann, J. Clendenin, T. Desikan, E. Garwin, R. Kirby, D. Luh, J. Turner, and R. Prepost, *Nucl. Instrum. Methods Phys. Res. A* **492**, 199 (2002).
- ²⁴T. Nishitani, T. Nakanishi, M. Yamamoto, S. Okumi, F. Furuta, M. Miyamoto, M. Kuwahara, N. Yamamoto, K. Naniwa, O. Watanabe, Y. Takeda, H. Kobayakawa, Y. Takashima, H. Horinaka, T. Matsuyama, K. Togawa, T. Saka, M. Tawada, T. Omori, Y. Kurihara, M. Yoshioka, K. Kato, and T. Baba, *J. Appl. Phys.* **97**, 094907 (2005).
- ²⁵W. Walukiewicz, J. Lagowski, L. Jastrzebski, and H. C. Gatos, *J. Appl. Phys.* **50**, 5040 (1979).
- ²⁶S. Tiwari and S. Wright, *Appl. Phys. Lett.* **56**, 563 (1990).
- ²⁷K. Togawa, T. Nakanishi, T. Baba, F. Furuta, H. Horinaka, Y. Kurihara, H. Matsumoto, T. Matsuyama, T. Nishitani, S. Okumi, T. Omori, C. Suzuki, Y. Takeuchi, K. Wada, K. Wada, M. Yamamoto, and M. Yoshioka, *Nucl. Instrum. Methods Phys. Res. A* **455**, 118 (2000).
- ²⁸J. E. Clendenin, A. Brachmann, E. L. Garwin, S. Harvey, J. Jiang, R. E. Kirby, D.-A. Luh, T. Maruyama, R. Prepost, C. Y. Prescott, and J. L. Turner, *Nucl. Instrum. Methods Phys. Res. A* **536**, 308 (2005).
- ²⁹M. Yamamoto, N. Yamamoto, S. Okumi, R. Sakai, M. Kuwahara, T. Morino, K. Tamagaki, A. Mano, A. Utsu, T. Nakanishi, C. Bo, T. Ujihara, Y. Takeda, and M. Kuriki, *AIP Conf. Proc.* **915**, 1025 (2007).
- ³⁰X. Jin, N. Yamamoto, Y. Nakagawa, A. Mano, T. Kato, M. Tanioku, T. Ujihara, Y. Takeda, S. Okumi, M. Yamamoto, T. Nakanishi, T. Saka, H. Horinaka, T. Kato, T. Yasue, and T. Koshikawa, *Appl. Phys. Express* (accepted).
- ³¹B. M. Dunham and L. S. Cardman, PAC 95 and IUPAP, 1996 (unpublished), Vol. 2, p. 1030.
- ³²S. Pastuszka, M. Hoppe, D. Kratzmann, D. Schwalm, A. Wolf, A. S. Jaroshevich, S. N. Kosolobov, D. A. Orlov, and A. S. Terekhov, *J. Appl. Phys.* **88**, 6788 (2000).